

Global Velocities and Positions Determined From GPS Data Spanning Three Years

Michael Heflin¹, Geoffrey Blewitt², David Jefferson
Yvonne Vigue¹, Frank Webb¹, and James Zumberge¹

¹Jet Propulsion Laboratory, California Institute of Technology

²The University of Newcastle upon Tyne

Abstract. Velocities and positions for 41 globally distributed sites have been determined from GPS data spanning three years. A no-fiducial approach has been developed to obtain these results without fixing any individual **positions** or velocities. Comparison with the ITRF92 velocity field, which was created from a combination of VLBI and SLR solutions, shows WRMS agreement at the level of 4.2 mm/yr, 5.7 mm/yr, and 7.4 mm/yr for geodetic latitude, longitude, and height rates respectively. Positions agree at the level of 6.8 mm, 10.9 mm, and 18.0 mm for latitude, longitude, and height.

Introduction

Very Long Baseline **Interferometry (VLBI)** and Satellite **Laser Ranging (SLR)** have been used to make precise geodetic measurements of position and velocity for over a decade (Ryan et al. 1993 and Smith et al. 1991). The **Global Positioning System (GPS)** represents a relatively new space-geodetic technique. The first global experiment using GPS took **place** in 1991. Baseline **precision** of 2 mm + 4 parts per billion was achieved without the **use** of fiducial constraints (Heflin et al. 1992) and positions were obtained with centimeter level accuracy (Blewitt et al. 1992). Here we present velocities and positions for 41 sites derived from GPS data spanning three years.

Analysis was carried out in four distinct steps. First, all daily site positions were estimated using weak constraints of 10 m to 1 km for each site component. Details of the analysis strategy are described by Heflin et al. (1992). Days for which GPS P-code encryption was in effect were not used. The number of receiver sites and satellites has increased significantly since 1991. The analysis strategy has also evolved with time. The most significant improvements include estimation of polar motion and UT1 rate along with a stochastic treatment of the satellite forces due to solar radiation pressure (Vigue et al. 1993). Second, all daily solutions were combined using a standard least-squares constant-velocity **model** to obtain a single set of positions and velocities. Third, internal constraints were applied instead of fiducial constraints. The basic idea of internal constraints is to fix several linear combinations of positions and velocities at their estimated values, instead of fixing some number of externally provided

positions and velocities. Finally, the estimated positions and velocities were transformed into the International Terrestrial Reference Frame for 1992 (1 TRF92). The no-fiducial approach used here is applicable to any global geodetic technique and is not specific to GPS. Various aspects of analysis are discussed more thoroughly below.

Transformation

When determining the positions of a set of points, an observer must choose a frame of reference. A terrestrial reference frame has an origin, a unit of length, and orientations for the three measurement axes. These reference frame parameters may be defined arbitrarily, but comparisons must take place in a particular frame. The origin is usually chosen to be the Earth's center of mass. The standard unit of length is the meter which is indirectly defined by the speed of light and the definition of a second. Approximately speaking, the z-axis points in the direction of the north pole, the x-axis is perpendicular to the z-axis, pointing toward Greenwich, England, and the y-axis is orthogonal to the other two axes in a right-handed sense.

Transformation from one reference frame to another has traditionally been accomplished with a seven-parameter **Helmert** transformation. Let upper and lower-case letters denote coordinates in two different frames. The **Helmert transformation** is written as

$$\begin{pmatrix} \mathbf{x} \\ \mathbf{y} \\ \mathbf{z} \end{pmatrix} = \begin{pmatrix} \mathbf{T}_x \\ \mathbf{T}_y \\ \mathbf{T}_z \end{pmatrix} + \begin{pmatrix} 1+S & -R_z & R_y \\ R_z & 1+S & -R_x \\ -R_y & R_x & 1+S \end{pmatrix} \begin{pmatrix} \mathbf{X} \\ \mathbf{Y} \\ \mathbf{Z} \end{pmatrix} \quad (1)$$

where parameters R_x , R_y , and R_z are **small angle** rotations, T_x , T_y , and T_z are translations, and S represents a small change in the unit of length. Differentiating both sides gives the corresponding velocity equation.

$$\begin{pmatrix} \dot{\mathbf{x}} \\ \dot{\mathbf{y}} \\ \dot{\mathbf{z}} \end{pmatrix} = \begin{pmatrix} \dot{\mathbf{T}}_x \\ \dot{\mathbf{T}}_y \\ \dot{\mathbf{T}}_z \end{pmatrix} + \begin{pmatrix} 1+S & -R_z & R_y \\ R_z & 1+S & -R_x \\ -R_y & R_x & 1+S \end{pmatrix} \begin{pmatrix} \dot{\mathbf{X}} \\ \dot{\mathbf{Y}} \\ \dot{\mathbf{Z}} \end{pmatrix} + \begin{pmatrix} \dot{S} & -\dot{R}_z & \dot{R}_y \\ \dot{R}_z & \dot{S} & -\dot{R}_x \\ -\dot{R}_y & \dot{R}_x & \dot{S} \end{pmatrix} \begin{pmatrix} \mathbf{X} \\ \mathbf{Y} \\ \mathbf{Z} \end{pmatrix} \quad (2)$$

Each transformation **parameter** now has a rate, doubling the total number from **seven** to fourteen (Heflin et al. 1993). A similar transformation without the scale rate parameter was independently derived by the International Earth Rotation Service (IERS) and used to create the ITRF92 velocity field (Boucher, Altamimi, and Duhem 1993).

In order to see the meaning of **these** parameters more clearly, consider two observers measuring the positions and velocities of a single set of points. There are three rotations because the observers' measurement axes may be facing in slightly different direction... The three rotation rates correct for the fact that the axes may be rotating slightly relative to one another, There are three translations because the observers' origins may be offset from one another. The three translation rates correct for any drift of the origins relative to one another. The **scale** parameter accounts for the fact that the **observers** maybe using slightly different **rulers** and the scale rate corrects for a small change in the relative lengths of the rulers. Once the transformation parameters are known, two **observers** can use the above **equations** to transform their measurements into a common reference frame for comparison.

The two observers can use their two sets of positions and velocities to estimate the transformation parameters, Let the lower-case letters represent measurements made by one observer and the upper-case letters represent measurements made by the other. When there are many sites, the **Helmert transformation** equation can be rearranged and written as

$$\begin{pmatrix} x_1 - X_1 \\ y_1 - Y_1 \\ z_1 - Z_1 \\ \vdots \end{pmatrix} = \begin{pmatrix} 1 & 0 & 0 & 0 & X_1 & 0 & Z_1 & -Y_1 \\ 0 & 1 & 0 & Y_1 & -Z_1 & 0 & X_1 & 0 \\ 0 & 0 & 1 & Z_1 & Y_1 & -X_1 & 0 & 0 \\ \vdots & \vdots & \vdots & \vdots & \vdots & \vdots & \vdots & \vdots \end{pmatrix} \begin{pmatrix} T_x \\ T_y \\ T_z \\ 0 \\ \dot{x} \\ R_y \\ R_z \end{pmatrix} \quad (3)$$

We can rewrite this equation as simply

$$AX = AX \theta_x \quad (4)$$

by defining AX as the vector of coordinate differences, AX as the matrix, and θ_t as the vector of **transformation** parameters. Differentiate both sides to get the corresponding velocity equation.

$$\dot{\Delta}_x = \dot{A}_x \theta_t + A_x \dot{\theta}_t \quad (5)$$

Now write both equation.. together.

$$\begin{pmatrix} \Delta_x \\ \dot{\Delta}_x \end{pmatrix} = \begin{pmatrix} A_x & 0 \\ \dot{A}_x & A_x \end{pmatrix} \begin{pmatrix} \theta_t \\ \dot{\theta}_t \end{pmatrix} \quad (6)$$

Simplify the notation once again by defining \mathbf{A} as the vector of position and velocity differences, \mathbf{A} as the full matrix, $\boldsymbol{\theta}$ as the vector of all fourteen transformation parameters, and adding a measurement noise term.

$$\Delta = \mathbf{A} \boldsymbol{\theta} + \mathbf{v} \quad (7)$$

Notice that the matrix \mathbf{A} relating the transformation parameters to the coordinate differences is constructed from the positions and velocities of **all** sites. Matrix \mathbf{A} will **come up again** during the discussion of internal constraints.

The transformation parameters are estimated using the weighted least-squares solution

$$\hat{\boldsymbol{\theta}} = \left(\mathbf{A}^T \mathbf{C}_{\Delta}^{-1} \mathbf{A} \right)^{-1} \mathbf{A}^T \mathbf{C}_{\Delta}^{-1} \Delta \quad (8)$$

with **covariance** matrix

$$\mathbf{C}_{\hat{\boldsymbol{\theta}}} = \left(\mathbf{A}^T \mathbf{C}_{\Delta}^{-1} \mathbf{A} \right)^{-1} \quad (9)$$

where

$$\mathbf{C}_{\Delta} = \mathbf{C}_x + \mathbf{C}_X \quad (10)$$

is simply the sum of the **covariance** matrices from each observer.

Internal Constraints

The idea of internal constraints is to constrain several linear combinations of positions and velocities at their estimated values instead of fixing some number of **position** and velocity components at externally provided values. Internal constraints offer two advantages. First, they **allow** the GPS estimates to remain independent of other techniques and second, they avoid the possibility of systematic effects due to errors in the externally provided information. The fourteen linear combinations being constrained were chosen to have a **one-to-one** correspondence with the fourteen **reference** frame parameters, so the effect of internal constraints is to fix the

reference frame parameters at their estimated values. The reader is referred to **Vanicek** and Krakiwsky (1986) for a complete mathematical derivation of internal constraints. Suffice it to say that we have generalized their formulation to include fourteen constraints and allow those constraints to be non-zero so that the final matrix is **fully** invertible. The resulting equations are given below.

Consider a set of positions and velocities represented by vector **X** with **covariance** matrix **C**. The matrix **A** discussed above can be computed from the elements of **X** and then used to obtain

$$B = (A^T A)^{-1} A^T. \quad (11)$$

Matrix **B** specifies which linear combinations **will** be constrained, Let the diagonal matrix **C₀** contain non-zero constraints for each of the fourteen parameters, These constraints are applied using

$$C_{\text{constrain}} = C - C B^T (B C B^T + C_0)^{-1} B C. \quad (12)$$

Although the above equation is valid when **C₀** is zero, small but non-zero constraints are used so that the new **covariance** matrix is invertible.

$$C_{\text{constrain}}^{-1} = C^{-1} + B^T C_0^{-1} B \quad (13)$$

The **constrained covariance** matrix gives reasonable errors for the position and velocity estimates.

Results

In summary, daily estimates were computed, combined, internally constrained, and then transformed into **ITRF92**. The estimated translation and scale parameters obtained were

$$\begin{aligned} S &= -1.3 \pm 0.4 \text{ ppb}, \dot{S} = -0.3 \pm -0.2 \text{ ppb/yr} \\ TX &= -1.4 \pm 0.3 \text{ cm}, \dot{TX} = 2.3 \pm -0.2 \text{ cm/yr} \\ T_y &= 4.2 \pm 0.3 \text{ cm}, \dot{T}_y = -5.4 \pm 0.2 \text{ cm/yr} \\ T_z &= -1.6 \pm -0.2 \text{ cm}, \dot{T}_z = -4.0 \pm 0.1 \text{ cm/yr} \end{aligned} \quad (14)$$

The unit of length as defined by **GPS** differs by about 1 ppb from that used for **ITRF92** and the estimated scale rate is not significant, The **GPS** determination of the center of mass is offset from the **ITRF92** value by several cm and is drifting by several cm/year. The **GPS** determination of the center of mass

is currently limited by the ability to model forces on the satellites such as those due to solar radiation pressure. The error bars above only reflect the contribution from ITRF92 because the internal constraints fix the GPS scale and origin at their estimated values.

The resulting **global** GPS velocity field is shown in Figure 1. Tectonic motion is clearly visible on the map. Spreading between the North American and Eurasian plates, slip between the Pacific and North American plates, convergence of the Pacific and Eurasian plates, and the northward drift of the Australian plate are clearly evident. More detailed interpretation by fitting a plate motion **model** is left as future work. The numerical estimates of position and velocity are given for July 1, 1992 in Table 1. Three sigma formal errors are used for all tables and figures. The sites GOLO, JPLO, and PINO, represent positions and velocities before the 92JUN28 Landers earthquake. The positions for BRMU, CANB, FORT, GOLO, GOLD, **HOB**A, KOUR, MADR, METS, and WETB refer to the top of the antenna. Positions for all other sites refer to the GPS monument location.

In addition to the qualitative agreement with known tectonic motion, a **rigorous** test is provided by comparison with the ITRF92 velocity field, Figure 2 shows comparisons of the GPS estimates for geodetic latitude, longitude, and height rate with those from ITRF92 which represent a combination of VLBI and SLR solutions. The WRMS differences are 4.2 **mm/yr**, 5.7 **mm/yr**, and 7.4 **mm/yr** for the latitude, longitude, and height rates respectively. A similar comparison for positions gives WRMS differences of 6.8 mm, 10.9 mm, and 18.0 mm. Of course, many sites are not collocated with VLBI or SLR, so their estimates represent new information which can be used to test models of plate motion and plate rigidity, as **well** as provide a **global** framework in which regional experiments can take place.

Acknowledgements. This research was partially carried out by the Jet Propulsion Laboratory, California Institute of Technology, under contract with the National Aeronautics and Space Administration. We thank the numerous institutions and individuals who operate the GPS constellation and global receiver network,

References

- Blewitt, G., M. Heflin, W. Bertiger, F. Webb, U. Lindqwister, and R. Malla, Global Coordinates With Centimeter Accuracy In The International Terrestrial Reference Frame Using The Global Positioning System, *Geophys. Res. Lett.*, Vol. 19, No. 9, 853-856, 1992.
- Boucher C., Z. Altamimi, and L. Duhem, ITRF 92 and its Associated Velocity Field, *IERS Technical Note 15*, IERS Central Bureau, Observatoire de Paris, 1993.
- Heflin, M., W. Bertiger, G. Blewitt, A. Freedman, K. Hurst, S. Lichten, U. Lindqwister, Y. Vigue, F. Webb, T. Yunck, and J. Zumberge, Global Geodesy Using GPS Without Fiducial Sites, *Geophys. Res. Lett.*, Vol. 19, No. 2, 131-134, 1992.
- Heflin, M., Generalized No-fiducial Approach to Global Geodesy, IOM 225.4-93-013 (JPL Internal document), Jet Propulsion Laboratory, California Institute of Technology, Pasadena, CA, 1993.
- Heflin, M., G. Blewitt, D. Jefferson, Y. Vigue, F. Webb, J. Zumberge, D. Argus, J. Gipson, and T. Clark, Global Positions and Velocities from One Year of GPS Data, *EOS Vol. 74, No. 4?*, 194, 1993.
- Smith, D., R. Kolenkiewicz, P. Dunn, J. Robbins, M. Torence, S. Klosko, R. Williamson, E. Pavlis, N. Douglas, and S. Fricke, Tectonic Motion and Deformation From Satellite Laser Ranging to Lageos, *J. Geophys. Res.*, 95(B13), 22013-22042, 1991.
- Ryan, J., C. Ma, and S. Caprette, NASA Space Geodesy Program-GSFC Data Analysis-1992, CDP VLBI Geodetic Results 1979-91, *NASA Technical Memorandum 104572*, GSFC, Greenbelt Maryland, 1993.
- Vigue, Y., S. Lichten, R. Muellerschoen, G. Blewitt, and M. Heflin, Improved Treatment of GPS Force Parameters in Precise Orbit Determination Applications, *Paper AAS 9.?-159, AAS/AIAA Spaceflight Mechanics Meeting, 1993.*
- Vanicek, P. and E. Krakiwsky, Geodesy, the concepts, Elsevier Science Publishers B. V., The Netherlands, 271-381, 1986.

Michael **Heflin**, David Jefferson, Yvonne **Vigue**, Frank Webb, and James **Zumberge**, Jet Propulsion Laboratory, MS 238--600,4800 Oak Grove Drive, Pasadena, CA 91109.

Geoffrey **Blewitt**, The University of Newcastle upon Tyne, Department of Surveying, Newcastle upon Tyne, NE1 7RU, England

(Received January ##, 1994;
Revised ##### ##, 1994;
Accepted ##### ##, 1994)

Copyright 1994 by the American Geophysical Union.

Paper number #####.
~~#####/###/###-#####~~\$03.00

Heflin et al.: Global GPS Velocity Field

Heflin et al.: Global GPS **Velocity** Field

Heflin et al.: **Global** GPS Velocity Field

Figure 1. Global GPS Velocity Field

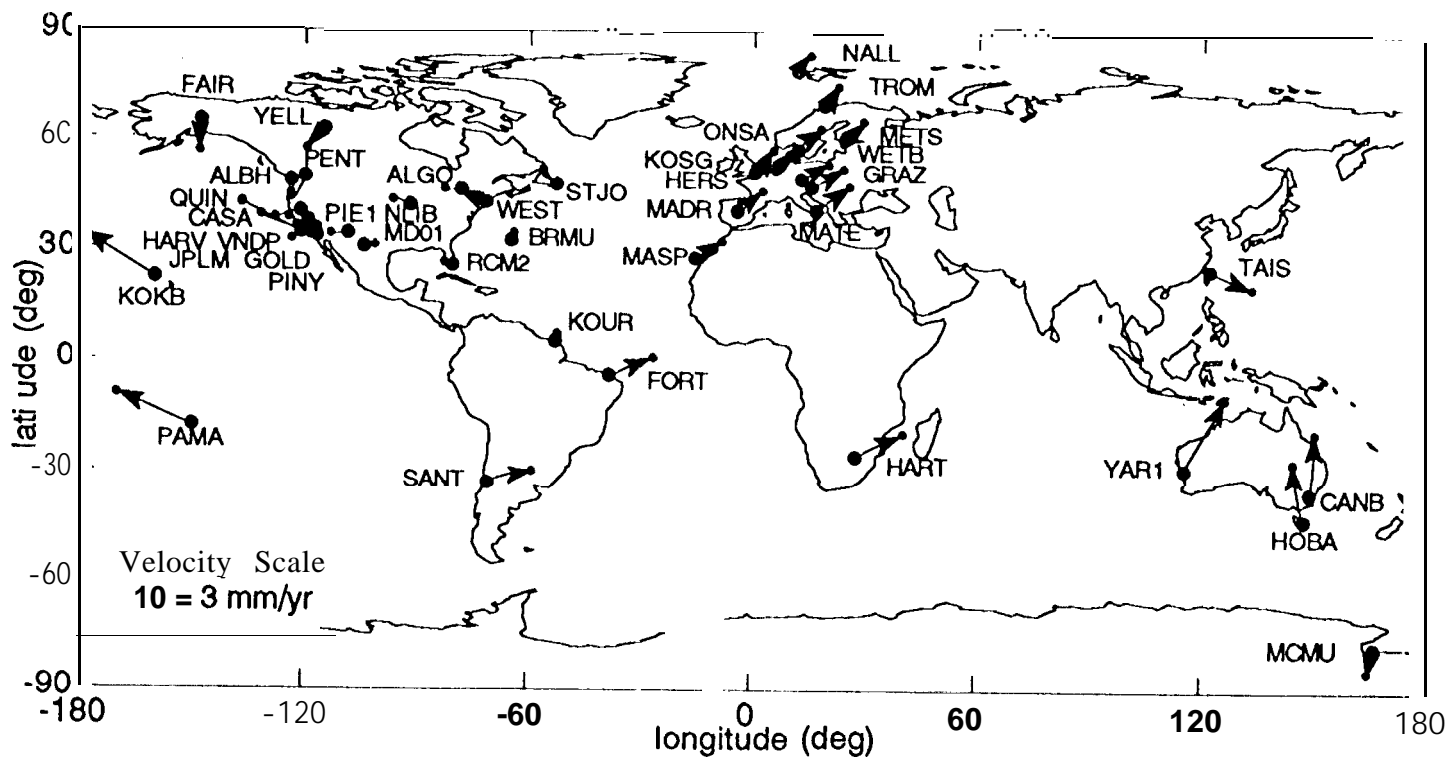
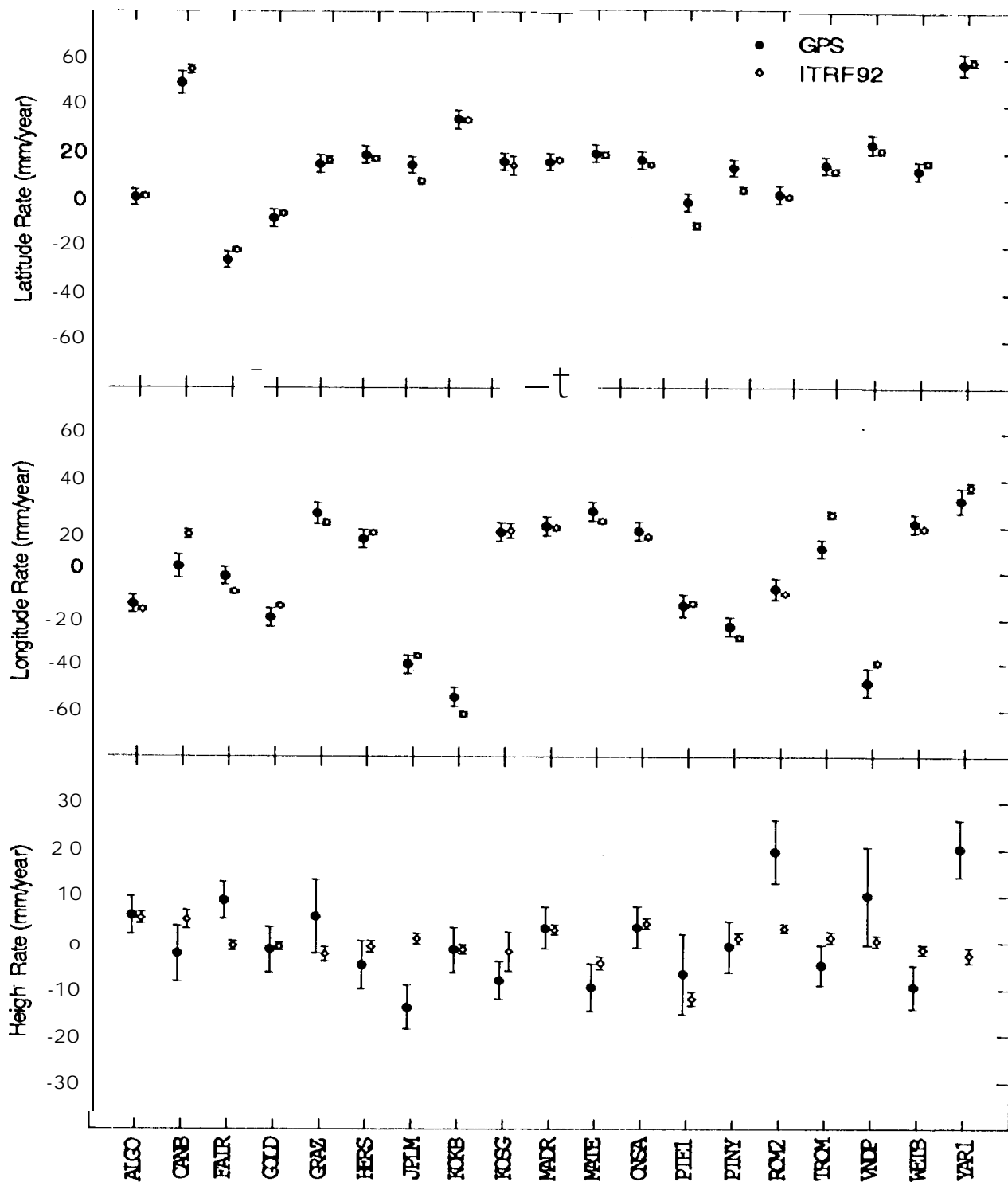


Figure 2, Comparison of GPS and ITRF92 Velocity Estimates



WRMS differences 4.2 mm/yr, 5.7 mm/yr, and 7.4 mm/yr for latitude, longitude, and height.

'T'able 1. GPS Positions and Velocities

Name	x mm	Y mm	Z mm	VX mm/yr	VY mm/yr	VZ mm/yr
ALBH	-2341332832* 2	-3539049508* 2	4745791399* 2	-7± 4	-11± 4	-6* 4
ALGO	918129591* 2	-4346071222* 2	4561977802* 2	-12* 4	-7* 4	4* 4
BRMU	2304703701* 9	-4874817264*14	3395186916*10	-4*10	14*14	-2*10
CANB	-4460996101* 4	2682557159* 3	-3674444003± 3	-24± 6	11± 5	41* 5
CASA	-2444430120* 8	-442868764(1*13	3875747386*10	-27* 9	-31± 13	26± 11
FAIR	-2281621325* 1	-1453595777* 2	5756961958* 2	-24* 4	-14* 4	-3± 4
FORT	4985387181*29	-3954999002*27	-42\$426612* 7	68*27	-9*26	10* 8
GOLO	-2353614103* 3	-4641385468* 5	3676976528* 4	-16* 5	5* 6	-7* 6
GOLD	-2353614110* 2	-4641385476* 2	3676976518* 2	-19* 4	5* 4	-7* 4
GRAZ	4194424051* 5	1162702475* 3	4647245270* 5	-14* 6	23± 5	14* 6
HART	5084625459* 6	2670366538* 5	-2768494025± 3	-8± 8	39* 7	16* 5
HARV	-2686069144* 4	-4527084488± 5	3589502240* 4	-35± 5	35* 6	19* 5
HERS	4033470300* 3	23672687* 2	4924301170* 3	-18* 4	15* 4	8* 5
HOBA	-3950183991*12	2522364466* 9	-4311588435*12	-22*12	25*10	35*12
JPLO	-2493304060* 3	-4655215570* 5	3565497343* 3	-34* 5	29* 6	3± 6
JPLM	-2493304062* 2	-4655215563* 3	3565497347* 2	-26* 4	36* 4	4* 4
KOKB	-5543838081± 3	-2054587551* 3	2387809576* 2	-6* 5	55± 4	31* 4
KOSG	3899225332* 2	396731747* 2	5015078299± 2	-19* 4	16± 4	4± 4
KOUR	3839591575* 6	-5059567676* 7	579956877* 2	6* 8	-6* 8	7* 4
MADR	4849202566* 2	-360329201* 2	4114913076* 2	-6* 4	21* 4	14* 4
MASP	5439189171* 4	-1522054857* 3	2953464202* 2	-1* 5	23± 4	12± 4
MATE	4641949817* 3	1393045201* 2	4133287271* 2	-27* 4	20* 4	9* 4
MCMU	-1310695213± 3	310468877* 3	-6213363449* 5	19* 5	1* 5	-7* 7
MDO1	-1329998628*15	-5328393405± 28	3236504221*17	14*14	22*26	-14± 16
METS	2892571046* 2	1311843291* 2	5512634067* 2	-20* 4	8* 4	4* 4
NALL	1202430727* 1	252626619* 1	6237767487* 3	-12* 4	7* 4	13* 5
NLIB	-130934391* 4	-4762291736* 8	4226854664* 7	-14* 6	-4* 9	10* 8
ONSA	3370658748* 2	711876969* 2	5349786824* 2	-16± 4	15* 4	12± 4
PAMA	-5245195125* 5	-3080472391± 5	-1912825513* 3	-41* 8	46± 7	22* 5
PENT	-2059164600* 1	-3621108398* 2	4814432419* 2	-16* 4	-5* 4	-8± 4
PIE1	-1640916710* 4	-5014781197* 6	3575447153* 4	-12* 5	9* 7	-4* 6
PI NO	-2369510386* 3	-4761207218* 5	3511396099* 3	-22± 5	19± 6	4* 6
PINY	-2369510359* 2	-4761207212* 3	3511396144* 3	-17* 4	18± 5	11* 4
QUIN	-251 7230895* 6	-4198595193* 9	4076531262* 8	-24* 7	-1* 10	5± 9
RCM2	961318983* 3	-5674090965± 5	2740489584* 3	-4* 5	-17* 6	11± 5
SANT	1769693271* 4	-5044574138* 5	-3468321 143* 4	24* 6	38* 7	30* 5
STJO	2612631332* 2	-3426807014* 2	4686757756* 2	-12* 4	-2* 4	12* 4
TAIS	-3024781857* 5	492\$936895* 5	2681234518* 3	-30* 6	-16± 7	-15± 5
TROM	2102940436* 2	721569344* 2	5958192076* 2	-18* 4	6* 4	1± 4
VNDP	-2678089764* 6	-4525437807* 8	3597431477* 6	-38± 6	29* 8	25* 7
WEST	1492233464* 5	-4458089422* 8	4296045927* 7	-17* 6	-15* 9	20± 8
WETB	4075578713* 2	931852621* 2	4801570051* 2	-20* 4	18* 4	1* 4
YAR1	-2389025328± 4	5043316830± 4	-3078530950* 3	-48* 5	28± 6	41* 5
YELL	-1 224452389* 1	-268921609]* 1	5633638285* 2	-21* 3	-11* 3	0* 4